Speeding up Heterogeneous Federated Learning with Sequentially Trained Superclients

Fault detection in level and flow rate sensors for safe and performant remote-control in a water supply system

Sofia Fellini, Riccardo Vesipa, Fulvio Boano and Luca Ridolfi

ABSTRACT

This work presents an algorithm for real-time fault detection in the SCADA system of a modern water supply system (WSS) in an Italian alpine valley. By means of both hardware and analytical redundancy, the proposed algorithm compares data and isolates faults on sensors through analysis of residuals. Moreover, the algorithm performs a real-time selection of the most reliable measurements for the automated control of the WSS operations. A coupled model of the hydraulic and remote-control system is developed to test the performance of the WSS when the proposed algorithm is applied or not. Simulations show that the occurrence of errors in the sensors causes significant worsening in the economic, energy and mechanical performance of the infrastructure. In many cases, the operations of the WSS are seriously compromised. The error detection and measurement assessment performed by the proposed algorithm proves to be crucial for the safe control of the WSS.

Key words | analysis of residuals, fault detection, optimal control, SCADA, water supply

Sofia Fellini (corresponding author)
Riccardo Vesipa
Fulvio Boano
Luca Ridolfi
Department of Environment, Land and Infrastructure Engineering,
Politecnico di Torino,
Corso Duca degli Abruzzi 24, 10129 Turin,
Italy
E-mail: *sofia.fellini@polito.it*

Sofia Fellini
Laboratoire de Mécanique des Fluides et d'Acoustique, UMR CNRS 5509,
Université de Lyon, Ecole Centrale de Lyon, INSA Lyon,
Université Claude Bernard Lyon I, 36, avenue Guy de Collongue, 69134 Ecully,
France

INTRODUCTION

In north Italian mountainous and hilly areas, water supply (WS) to local communities is usually provided by municipal water supply systems (WSSs) that rely on local sources and operate independently from each other. In these regions, in fact, the availability of water resources is generally not an issue, and the high degree of territorial dispersion favors a decentralized water management. In the event of unexpected breakdowns or droughts (Carrera *et al.* 2013), however, this fragmentation results in inefficiencies and water crises. In order to increase the resilience of the WS service, a growing trend is the creation of inter-municipal water networks that connect multiple local WSSs over large areas (Massarutto 2000). Coordination in the operations of multiple WSSs and diversification of water sources entail economic, environmental, and water quality advantages (Anghileri *et al.* 2012; Bel & Warner 2015), and they are in line with the principle of integrated water resources management pursued by the European Water Framework Directive (EC 2000).

Large-scale water infrastructures require an automated regulation aimed at controlling the operations of the entire system, according to a centralized control philosophy. For this reason, they are managed by SCADA (Supervisory Control and Data Acquisition) systems (e.g., Coelho & Andrade-Campos 2014; Meseguer & Quevedo 2017) that (i) acquire and analyze real-time pressure and flow rate measurements provided by sensors in the key points of the network, and (ii) remotely control the operations of the regulation devices (e.g., valves, pumps, turbines), according to predefined management rules and as a function of the data measured in real-time throughout the system.

In this framework, faulty sensors in the system may induce the SCADA to perform wrong regulations and, thus, result in faulty water supply system (WSS) operations. To ensure the robustness of the control operations, control systems have to be integrated with procedures that detect errors in sensors and activate in response actions for a safe management. This is crucial for large hydraulic

doi: 10.2166/hydro.2019.002

infrastructures that transfer and supply water over large and steep areas. These systems are particularly vulnerable to failures, as the large volumes of water and the high pressures involved can cause dangerous consequences when the system regulation is not optimal.

Fault detection and isolation (FDI) methods have been proposed in different fields of engineering and can be roughly classified into signal-based and method-based techniques (Gao *et al.* 2015).

Basic signal-based methods (e.g., Mourad & Bertrand-Krajewski 2002; Burnell 2003) evaluate data as valid or faulty by assessing the value or the variation of the signal. Advanced signal-based methods (e.g., Frank & Köppen-Seliger 1997; Maki & Loparo 1997) include techniques from machine learning, like neural networks. Signal-based methods are generally used when measurement redundancy is not available in the system, when the number of sensors under analysis is huge, and when a model of the system cannot be developed.

On the other hand, model-based methods validate data by using dependencies between different measurable signals. To this aim, both hardware redundancy or analytical redundancy (Hwang *et al.* 2010; Gertler 2015) can be exploited. In hardware redundancy, measurements of the same physical variable are acquired by redundant sensors and compared. Conversely, analytical redundancy uses a mathematical model of the system as a comparison term (Frank 1996; Isermann 2005). Hardware redundancy is commonly adopted in safety-critical systems (Goupil 2011), but it involves significant extra costs. Moreover, sensors tend to have a similar lifetime and thus sensors that were installed at the same time in the infrastructure often fail simultaneously. In large-scale systems, analytical redundancy represents a convenient alternative due to the number of sensors, and the high cost of their installation, interconnection, and maintenance (Boukhris *et al.* 2001). Fault detection in model-based methods involves two steps: (i) residual generation and (ii) residual evaluation. A residual is obtained as the difference between two redundant measurements. Its signal is ideally zero when the system is operating correctly and non-zero when faults are present. Residual evaluation is the set of techniques that correctly identify the occurrence of an error starting from the analysis of the residuals (Frank & Ding 1997).

FDI techniques have been widely studied in the field of control engineering, such as in industrial plants (e.g., Gertler 1988; Özyurt & Pike 2004) and in automotive and aerospace engineering (Chen & Patton 2012). In the hydraulic and hydrological field, applications of FDI involved the analysis and reconstruction of hydrological time-series (e.g., Quevedo *et al.* 2010), leak/burst detection in water distribution networks (e.g., Krause *et al.* 2008; Casillas *et al.* 2013), and problems related to water quality monitoring (e.g., Eliades & Polycarpou 2010). A few works instead dealt with the identification of faulty sensors for a safe remote control of WSSs. Among these, Gabrys & Bargiela (1996) determined confidence intervals for flow rate measurements by means of a neural network approach. Ragot & Maquin (2006) proposed a method based on fuzzy logic for measurement fault detection in an urban WSS. Izquierdo *et al.* (2007) applied a FDI hybrid method based on neural networks and fuzzy theory. Meseguer *et al.* (2010) and Cugueró-Escofet *et al.* (2016) used fault signature matrices to identify a faulty sensor by means of the effect that the wrong measurement transmitted by this sensor potentially has on the other variables measured in the system. These methods proved to be efficient but their implementation in real hydraulic systems requires a certain degree of control theory expertise and a relevant computational cost.

Starting from the work of Fellini *et al.* (2018), the goal of this paper is to present an easy-to-implement and robust algorithm for fault detection in the SCADA system of a modern WSS. To increase the safety and the reliability of the control system, measurements from sensors are assessed in real time. By the analysis of residuals, redundant measurements are compared, and faults are automatically detected. Moreover, in case of errors, the developed algorithm ensures continuity in the control operations and prevents interruptions in the water supply. In addition to the introduction of a new FDI method, tools for the application and validation of the algorithm in typical WSSs are also provided in this work. In this way, the application of the method to real WSSs is facilitated.

The work is organized as follows. After this introduction, the 'Materials and methods' section presents first the logic and the structure of the proposed algorithm for fault detection. Then, the application of the algorithm to a

modern and multipurpose WSS is illustrated. To conclude the 'Materials and methods' section, the developed tools for the validation of the proposed algorithm are described. In the 'Results' section, the performances of the WSS before and after the application of the fault detection method are assessed. Finally, the main conclusions obtained from the present work are drawn.

MATERIALS AND METHODS

Algorithm for fault detection in sensors

An easy-to-implement and robust method for real-time fault detection in the SCADA system of a WSS has been developed. This method is based on the redundancy concept and thus can be applied when different measurements of the same physical quantity are available.

Usually, critical sensors in a SCADA system are duplicated. However, double redundancy provides error detection but not recovery. In fact, if two different measurements are read by two redundant sensors, the supervisory system can easily detect the presence of an error but cannot automatically recognize which one is the faulty device. In this case, a technician's on-site intervention is the only solution to identify the problematic sensor, and this may lead to an interruption of the control operations of the WSS. In large-scale water infrastructures, this interruption is extremely unsafe.

To guarantee continuity in real-time control operations, a procedure for the automatic detection and correction of faulty measurements is thus required. This is achieved with an error detection system based on triple redundancy. In this case, if one of the three sensors fails, the other two sensors can isolate the faulty sensor and provide a useful and reliable measurement.

The algorithm we present detects faults by comparing three values of the same physical variable, provided by two redundant gauges (hardware redundancy) and by a hydraulic equation (analytical redundancy). In this way, resilience is achieved and the expensive installation of three redundant sensors is avoided.

In particular, the fault detection algorithm (Figure 1) receives as input three values (A, B, and C) of the same

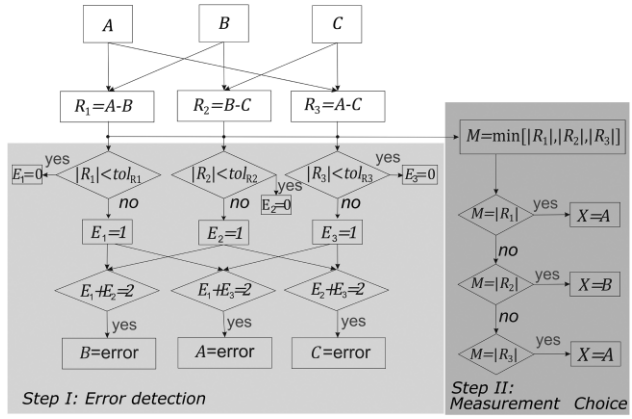

Figure 1 | Algorithm for fault detection (Step I) in a WSS sensors and for the choice of the most reliable measurement (Step II) to be used in the control operations.

observed variable (e.g., water level in a tank or flow rate along a pipe). A and B are transmitted by two redundant sensors, while C is obtained from a hydraulic balance. Residuals R_1, R_2, and R_3 are generated by calculating the difference between measurements two by two:

$$R_1 = A - B, \quad R_2 = B - C, \quad R_3 = A - C \tag{1}$$

Due to instrumental precision, random errors (see the 'Error modeling' section) are intrinsic in instrumental readings and therefore residuals are generally non-zero even if no errors are present. For this reason, faults are detected by comparing each residual to its tolerance. The tolerance intervals are defined in order to include precision errors, as:

$$tol_{R1} = tol_A + tol_B, \; tol_{R2} = tol_B + tol_C, \; tol_{R3} = tol_A + tol_C, \tag{2}$$

where tol_A, tol_B, and tol_C are the maximum instrumental errors expected for measurements A, B, and C, respectively. If the *i-th* residual exceeds its tolerance, the *i-th* error variable, E_i, switches to 1 (e.g., if $|R_1| > tol_{R1}$, $E_1 = 1$). When a sensor fails, two of the three error variables (E_1, E_2, and E_3 in Figure 1) assume value equal to 1, since the error associated with a single measurement appears in the calculation of two residuals. As a consequence, the algorithm can automatically detect which one is the faulty sensor (e.g., if R_1 and R_3 are out of tolerance, the sensor providing measurement A is identified as faulty).

Besides real-time error detection, the developed algorithm automatically selects the most accurate data to be

used in the control operations of the SCADA system (step II in Figure 1). For each set of three measurements (A, B, C), the minimum residual is identified (M in Figure 1). The two measurements involved in the calculation of M are the closest to each other and therefore considered the most representative of the real physical value. The algorithm selects one (X in Figure 1) of these two measurements as input for the control operations. This last choice is based on technical considerations. Generally, priority is given to direct measurements compared to indirect ones (i.e., those calculated from quantities different from the measured one). For example, in Figure 1, when $M = R_1$ the algorithm selects A as the input for the control operations. Measurement B would have been an equally correct datum but for technical reasons A is considered more reliable (e.g., A is directly given by a sensor while B is obtained from a hydraulic balance or from a sensor with lower instrumental precision).

The here-presented algorithm is designed for real-time applications. In remote-controlled WSSs, programmable logic controllers (PLC), networked to the SCADA systems, receive measurements from the sensors. The fault detection algorithm is implemented in the PLCs and evaluates the reliability of these measurements. Reliable measurements are thus selected by the algorithm and adopted for the management of the control devices (e.g., valves, turbines). The frequency for this measurement check is case specific. It can be lower than the data acquisition frequency but has to be higher than the frequency of the adjustment operations, and therefore of the rate of variation of the hydraulic properties in the system.

Application of the algorithm to a real WSS

The proposed algorithm for fault detection and measurement assessment is non-specific and applies to WSSs with three basic requirements: (i) a SCADA communication network collects measurements from sensors throughout the system; (ii) programmable logic controllers (PLCs) operate the control devices (e.g., valves, turbines) according to the dynamics of a number of measured variables (e.g., flow rates, tank levels); (iii) three independent measurements of each control variable can be obtained from redundant sensors or models. A case study is introduced to improve the understanding of the method, to present a real application, and to show some useful tools for its validation.

Case study

The case study is described in detail by Fellini *et al.* (2017) and involves a modern WSS (Figure 2) located in an Alpine valley in the northwest of Italy. The WSS consists of an 80-km-long water main connecting 20 municipal WSSs. The water main collects high quality water from an alpine reservoir and conveys a maximum flow rate of 500 l/s. The municipal WSSs (see the inset in Figure 2) are self-sufficient under ordinary conditions as they are supplied by local sources (springs and wells). However, they receive water from the water main when the local sources fail, their quality is low, or water treatment in local plants is expensive. Needle valves with electronic actuators regulate the flow delivered from the water main to the municipal tanks. In the upper valley, four inline tanks (S_1, S_2, S_3, and S_4) split the water main in order to limit the static water pressure in the pipes. A Pelton turbine with electronically controlled Doble needles adjusts the flow entering in each inline tank. In this way, hydropower generation is also performed.

Valves and turbines are the active elements that regulate the flow rate in the entire WSS. Local PLCs control these devices according to (i) predefined management rules, (ii) flow rate and level data measured by sensors installed near the regulation devices, and (iii) data received from the distant sensors networked in the SCADA system. Data transmission in the SCADA system is guaranteed by an optical fiber network.

The management rules of the active devices were developed to optimize water distribution and to maximize the hydropower generation and the energy saving in the entire system (Fellini *et al.* 2017). In particular, flow adjustment through the turbines is aimed at (i) maintaining the water level in the inline tanks between two predefined level thresholds and (ii) minimizing the number of turbine operations. To this aim, turbines T_1 and T_2 are regulated according to the water level in the upstream tanks S_1 and S_2, respectively. An upper and a lower level threshold are predefined for each one of these tanks. When the water level crosses one of these thresholds, the status of the

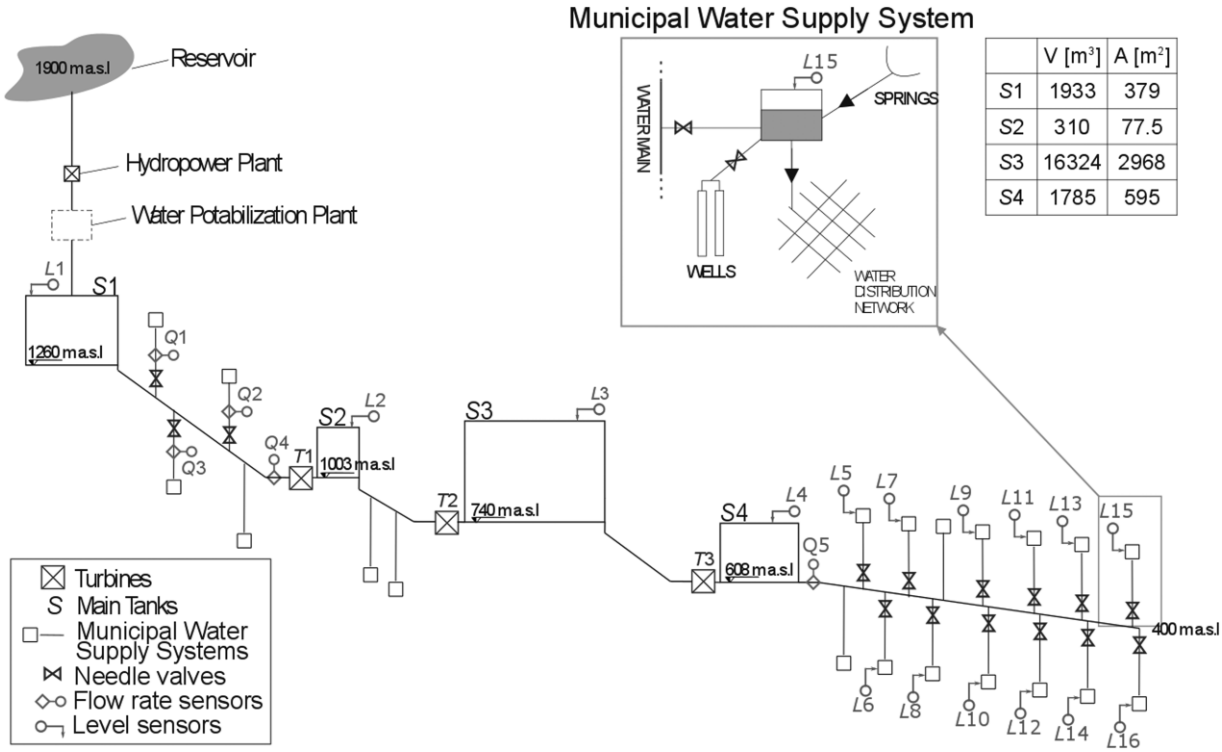

Figure 2 | Scheme of the WSS adopted as case study. The water main is split by four main tanks (the rectangles denominated S_1–S_4) and it supplies 20 municipal tanks (the small white squares). The inset shows a typical municipal water system with the storage tank supplied by mountain springs, local wells, and by the new water main. The flow rate and level sensors involved in the regulation operations are respectively represented as small diamonds and arrows overlaid by a circle. The control devices, i.e., needle valves and turbines, are depicted as 'bow tie' symbols and square with cross symbols.

downstream turbine is updated. The updated value (Q_T) of the flow rate through the turbine is calculated by the SCADA system in order to close the balance:

$$Q_T = Q_{IN} - \sum_i Q_{EX,i} \tag{3}$$

where Q_{IN} is the flow rate entering the tank and $Q_{EX,i}$ is the flow rate supplied to the *i-th* municipal WSS along the pipeline segment between the tank and the turbine. Q_T value is rounded up when the crossed threshold is the higher one. It is rounded down when the crossed threshold is the lower one. In this way, the water level slowly varies between the two thresholds and the number of turbine adjustments is minimized. An additional minimum threshold is set to avoid the emptying of the tank (i.e., to prevent air from entering the water main) in emergency conditions. When the water level falls below this threshold the downstream turbine is completely closed. The same rationale is used to control the flow rate through turbine T_3. However, the regulation is performed according to the water level in the downstream tank S_4. As a consequence, in Equation (3), the flow rate out of the tank (Q_5 in Figure 2) appears instead of Q_{IN}, and when the emergency threshold in tank S_4 is crossed, turbine T_3 is fully opened. The involved measurements for the control of the turbines are thus given by the level sensors in the inline tanks (L_1 to L_4) and by the flow rate sensors installed along the water main (e.g., Q_4 and Q_5) and along the pipes that supply the municipal tanks of the upper valley (e.g., Q_1 to Q_3).

The water level in the inline tank S_3 is instead used to control the flow rate towards the municipal tanks in order to optimize the distribution of water in the whole system. Tank S_3 has the largest capacity, and thus its level is an indicator of water availability in the system. According to L_3 dynamics and to a predefined priority list (based on technical and economic criteria), the municipal WSSs to be supplied by the water main are selected. Alternatively, the municipal tanks are supplied by the local wells. In both

cases, the flow rate to the municipal tank is proportional to the tank water level. As for the inline tanks, an emergency level threshold is set for the municipal tanks. When the water level falls below this threshold, the water main supplies the tank with a predefined constant flow rate. The involved measurements for the control of the needle valves are thus given by level sensors in the municipal tanks (e.g., L_5 to L_{16}) and by L_3.

Notice that all the municipal WSSs are actually provided with meters. However, the level and flow rate sensors of four of them are not shown in Figure 2. These sensors are not considered in the simulations discussed in the following sections because the management rules in which they are involved are rather specific.

Assessment of hardware and analytical redundancy in the system

The above-presented fault isolation procedure is effective if three measurements A, B, and C of the same physical quantity are available. As introduced in the 'Case study' section, the key quantities for the control operations are: (i) water levels in the inline tanks (L_1 to L_4 in Figure 2) and in the municipal tanks (L_5 to L_{16}); and (ii) flow rates along the water main (Q_4 and Q_5) and towards the municipal WSSs in the upper valley (Q_1 to Q_3).

Regarding level measurements, each tank is equipped with two redundant level sensors (MH_1 and MH_2 in Figure 3(a)). Moreover, the tank level can be evaluated with a mass balance equation that estimates the actual tank level (C in Figure 3(a)) as a function of the tank level in the previous time step (Δt), the tank area (A_T), and the flow rates into and out of the tank (MQ_{IN} and MQ_{OUT} in Figure 3(a)):

$$C(t) = C(t-\Delta t) + [MQ_{IN}(t-\Delta t) - MQ_{OUT}(t-\Delta t)]\frac{\Delta t}{A_T} \quad (4)$$

Notice that this balance is independent from the level measurement sent by sensors MH_1 and MH_2. Otherwise, any error in one of the two level sensors would also propagate within C and the error identification method would fail.

Regarding flow rate measurements towards the municipalities, two flow meters are installed along the pipes that supply each municipal tank. Generally, one is installed near the tank and the other at the connection to the water main (MQ_1 and MQ_2 in Figure 3(b)). Furthermore, some flow meters intercept the water main (MQ_A and MQ_B in Figure 3(b)). Thus, a third value (C) of the flow rate towards each one of the local WSSs can be evaluated with the following flow rate balance equation:

$$C(t) = MQ_A(t) - MQ_B(t) \quad (5)$$

Finally, for the flow rates along the water main (Q_4 and Q_5 in Figure 2), redundant flow rate sensors at the entrance and at the exit of the inline tanks are installed (Figure 3(c)). The flow rate balance (Equation (5)) is used to compute the third redundant measurement.

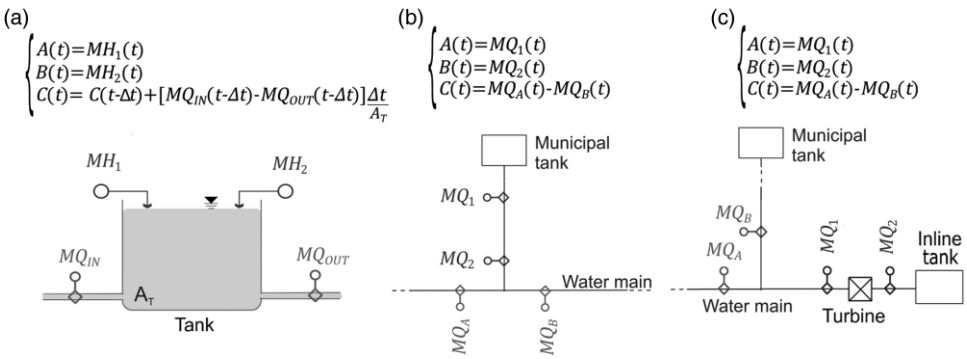

Figure 3 | (a) Level (MH_1 and MH_2) and flow rate (MQ_{IN} and MQ_{OUT}) sensors installed in the tanks (with area A_T) of the WSS. The system of equations provides three redundant values (A, B, and C) of the tank level. (b) Flow rate sensors installed along the pipe that supply the municipal tanks (MQ_1 and MQ_2) and along the water main (MQ_A and MQ_B). The system of equations provides three redundant values (A, B, and C) of the flow rate towards the municipal tank. (c) Flow rate sensors installed at the entrance of the inline tanks (MQ_1 and MQ_2), along the water main (MQ_A), and along the pipes that supply the municipal tanks (MQ_B). The system of equations provides three redundant values (A, B, and C) of the flow rate into the inline tank.

Tolerance intervals for the residuals

In the proposed error detection algorithm, a tolerance interval for each residual has to be defined. Within this interval the residual is accepted. The tolerance interval is obtained from the sum of the maximum precision errors expected for the two measurements involved in the calculation of the residual, i.e., a combination of two between tol_A, tol_B, and tol_C (see Equation (2)).

For flow rate measurements (Figure 3(b) and 3(c)), tol_A and tol_B are set as the maximum instrumental error (E_{max}) of the installed flow meters. tol_C is the maximum precision error expected for the indirect estimation (C) of the flow rate. Equation (5) defines C as a linear combination of flow rate measurements MQ_A and MQ_B. For this kind of indirect measurement, the uncertainty is determined by the law of propagation of uncertainty (JCGM 2008). In the case of linear models, the law of propagation states that the variance of an indirect measurement is given by a quadratic combination of the variance of the directly measured quantities. Referring to Equation (5), the variance of C reads:

$$\sigma_C^2 = \sigma_{MQ_A}^2 + \sigma_{MQ_B}^2 \tag{6}$$

Assuming a Gaussian distribution for the measurement results, the maximum precision error can be estimated as three times the standard deviation. As a consequence, tol_C becomes:

$$tol_C = 3\sigma_C = 3\sqrt{\sigma_{MQ_A}^2 + \sigma_{MQ_B}^2} \tag{7}$$

where the variance of the flow rate measurements MQ_A and MQ_B is obtained as a function of their maximum instrumental error:

$$\sigma_{MQ_A}^2 = \left(\frac{E_{max,MQ_A}}{3}\right)^2, \quad \sigma_{MQ_B}^2 = \left(\frac{E_{max,MQ_B}}{3}\right)^2 \tag{8}$$

Similarly, for level measurements (Figure 3(a)), tol_A and tol_B are set as the maximum instrumental error stated for the installed level sensors (MH_1 and MH_2). tol_C is the maximum precision error expected for the indirect estimation of the tank level, obtained from the mass balance in Equation (4). Considering the law of propagation of uncertainty, tol_C for the level measurement at time t reads:

$$\begin{aligned} tol_{C,t} &= 3\sigma_{C,t} \\ &= 3\sqrt{\left(\frac{tol_{C,t-\Delta t}}{3}\right)^2 + (E_{max,MQ_{IN}}^2 + E_{max,MQ_{OUT}}^2)\left(\frac{\Delta t}{3\,A_T}\right)^2} \end{aligned} \tag{9}$$

In Equation (9), tol_C increases with each time step. To avoid this progressive growth of the tolerance range and to keep it significant in the validation process, tol_C is forced equal to tol_A when it exceeds a threshold value equal to twice the tolerance of the installed level sensors (e.g., tol_A).

Kalman filters (e.g., Piatyszek *et al.* 2000; Ciavatta *et al.* 2004) could be used alternatively to Equations (4) and (9) to produce an estimate of the variable C, with its uncertainty σ_C. However, to reduce the uncertainty related to the modeled variable C, Kalman filters require a recursive update of the estimated variable based on the real value measured by a sensor. In the method proposed in this work, however, C has to be independent from the measured values (i.e., A and B). For this reason, the implementation of Kalman filters is here avoided.

Figure 4 shows the residuals R_1, R_2, and R_3 and their tolerance intervals (see Equations (1) and (2)) for the assessment of the level measurement in tank S_1. The tolerance

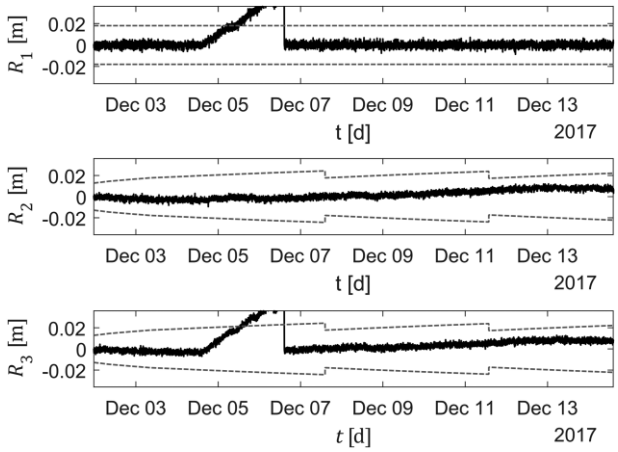

Figure 4 | Residuals (continuous lines) and their tolerance intervals (dashed lines) for level measurement in tank S_1. Level sensor MH_1 is affected by drift. Consequently, residuals R_1 and R_3 present a drifted signal and exceed their respective tolerance ranges. The tolerance intervals of residuals R_2 and R_3 are not constant as they are a function of tol_C (see Equation (9)). Q7

interval of residuals R_2 and R_3 (tol_{R2} and tol_{R3}) present a trend of interrupted growth as R_2 and R_3 are a function of tol_C. In the proposed example, the level sensor MH_1 is affected by drift (see section 'Error modeling'). As a consequence, residuals R_1 and R_3 exceed their tolerance intervals and the sensor malfunction is detected.

In the considered WSS, flow rate is measured by electromagnetic flow meters with a maximum instrumental error (E_{max}) equal to 0.25% of the flow rate in transit, while levels are measured by ultrasonic level sensors with E_{max} equal to 0.15% of the full-scale (this latter is equal to 6 meters).

Tools for the validation of the fault detection algorithm

The efficacy of the proposed algorithm in detecting errors in sensors is assessed through numerical simulations. To perform these simulations, a numerical model of the hydraulic and control operations is developed, and realistic errors in sensors are simulated. To assess in a quantitative way the performance of the WSS under the different simulated scenarios, custom performance indexes are introduced.

Hydraulic and control model

A simulation model was developed to analyze the performances of the WSS in different scenarios (Fellini *et al.* 2017). This model consists of a coupled hydraulic and control model.

The hydraulic model is a system of non-linear equations describing (i) the flow-head loss relation in pipes, at valves and at turbines, (ii) the flow continuity at nodes, and (iii) the boundary conditions at tanks. Time evolution of the system is modeled by a succession of steady states with duration Δt. At each time step, the flow in the pipes and the pressure at nodes are computed. Moreover, the water level in tanks is updated using a mass balance equation.

The control model simulates the supervision and control operations of the SCADA system. A measurement from each one of the installed sensors is modeled as $m = M + \epsilon$, where M is the flow or level computed by the hydraulic model at the exact point where the sensor is located. This value is perturbed with the error ε to model different kinds of sensor faults. These measurements are used as input data for the decision-making algorithms that simulate the control actions of the SCADA system, that is, the governance of valves and turbines.

Error modeling

Measurement errors are of different types and originate from different causes. In this work, we simulate errors that usually affect meters in monitoring systems (Balaban *et al.* 2009; Sharma *et al.* 2010). These are: random errors, instrumental drifts, sensor breakdowns and interruption of signal transmission (Table 1).

Random errors (also called statistical errors) are intrinsic errors that depend on the precision limitation of the measurement devices (e.g., Fuller 2009). In the simulated control system, random errors are modeled as realizations of a Gaussian distribution with mean equal to zero and with a standard deviation that depends on the instrumental precision. In particular, according to the three-sigma rule (Pukelsheim 1994), we estimate the standard deviation as one-third the maximum instrumental error (E_{max}).

Instrumental drift is a progressive bias in the measurement output which increases slowly in time (e.g., Webster

Table 1 | Types of considered errors in sensors and their simulation in the control model of the WSS

Type of error	Subtype	Error simulation
Random error	–	Gaussian distribution with $\mu = 0$ and $\sigma = E_{max}/3$
Drift	*Zero drift*	Instrument calibration curve with intercept increasing over time from 0 to 20% of the instrument full-scale
	Sensitivity drift	Instrument calibration curve with angular coefficient increasing over time from 1 to 1.2
Breakdown	*Minimum constant value*	Zero constant value
	Maximum constant value	Constant value stuck at the instrument full-scale
	Abrupt oscillations	Binomial distribution taking value 0 or the instrument full-scale with equal probability 0.5
Loss of signal	–	NaN

1998). It is caused by various environmental issues and by mechanical wear. In unaltered meters, the relation between the input (i.e., the value of the physical variable) and the output (i.e., the measurement) of the measurement process is a bisector. When this ideal bisector moves vertically, i.e., the instrument output has an offset with respect to the input, the meter is affected by 'zero drift'. This offset may increase over time. When the angular coefficient of the bisector changes over time, the sensor is affected by 'sensitivity drift'. In the simulated control model, the calibration curve of the instrument is disturbed by (i) an increase of the offset from zero to 20% of the instrument full-scale occurring over 10 days, and (ii) by a 20% increment of the angular coefficient over the same period.

Sensor breakdowns are usually caused by mechanical damage or electrical issues in internal connections. In the event of a breakdown, the operation of the meter is compromised, and the measured quantity deviates completely from the measured physical variable, i.e., the sensor output is usually stuck at a constant value equal to the full-scale of the instrument or to the minimum detectable value. Alternatively, the measure oscillates unstably between these two values. Stuck sensors are simulated in the control model by setting the measured value on the minimum detectable value or on the full-scale of the instrument. Unstable oscillations are generated through a random extraction over time between these two extremes.

Loss of signal is a complete loss of sensor data, due to a failure in the sensor or in the transmission network. In this case, the sensor output is simulated as a NaN (i.e., Not a Number).

Performance indexes

To analyze the operations of the hydraulic system in scenarios with different failures of the sensors, we introduce four performance indices. The first one is a normalized index of the time to breakdown, calculated as:

$$IT = \frac{T_{fin}}{T_{sim}} \tag{10}$$

where T_{fin} is the time in which the WSS operates without criticalities (i.e., empty conditions in the tanks), while T_{sim} is the total simulation time (one month). If $IT < 1$, errors in sensors are responsible for the failure of the WSS.

For the simulations with $IT = 1$, three additional normalized indexes are calculated. As detailed in the 'Case study' section, the aim of the studied WSS is to supply high quality water and to generate hydropower electricity. Thus, to analyze the performance of the system we calculate the performance quantities

$$E = \text{Net Energy} = E_T - E_P \tag{11}$$

$$W = \text{Lost water} = Vol_{over} \tag{12}$$

$$M = \text{Number of turbine operations} = n_{T1} + n_{T2} + n_{T3} \tag{13}$$

E_T and E_P are respectively the energy generated by the three turbines and the energy absorbed by the pumping plants that supply the local tanks. The difference between these two quantities corresponds to the green net energy produced by the system. Vol_{over} is the total volume of overflown water at tanks. When water flows are not properly governed, this parameter is greater than zero and quantifies the lost water in the system. n_{T1}, n_{T2}, and n_{T3} are the number of flow adjustments in the three turbines. For the hydraulic stability of the control devices (Vesipa & Fellini 2019) and for mechanical weariness, this parameter is optimal when minimized.

These metrics are compared with those obtained for the benchmark simulation, that is, the simulation of an ideal behavior of the system, with optimal measurement acquisition by the sensors. This simulation is a reference for the other scenarios and is hereinafter referred to as the benchmark ('B'). The following normalized indexes can thus be defined:

$$IE = \frac{E}{E_B},\ IW = \frac{W_{max} - W}{W_{max}},\ IM = \frac{M_B}{M} \tag{14}$$

where W_{max} is the maximum lost water among all the simulations. These indexes are equal to 1 when the performance of the disturbed system is the same as in the benchmark case. Indexes tend to zero as the system performance worsens due to faulty sensors. The water index (IW) is always between 0 and 1 since the lost water in the benchmark simulation is zero. Index IE(IM) can take values greater than 1, if

the net energy produced (the number of turbine operations) is higher (lower) than in the benchmark simulation. However, even if one of the indices is greater than 1, the overall performance of the WSS is always expected to be worse than in the benchmark case.

RESULTS

Numerical simulations of the WSS operations are performed to (i) analyze the effects of the transmission of faulty measurements from the meters to the telecontrol system and (ii) verify the efficiency of the error identification algorithm.

First, we simulate the operation of the WSS in the case of errors in the sensors and complete lack of measurement redundancy. Then, the error identification algorithm is introduced into the control model, the same error scenarios are reproduced, and the resilience of the system is investigated.

In these analyses, only the measurements that are essential for the WSS control operations are considered. These measurements are: the water level in the inline and municipal tanks (L_1–L_{16}) and the flow rate along the water main and towards the municipal tanks of the upper valley (Q_1–Q_5). In Figure 2 and in the 'Case study' section, details are given about the location of these measurements and how they are involved in the control operations.

For each of these measurements, three different kinds of errors are simulated: (i) drift, (ii) constant minimum value, and (iii) constant full-scale value. Moreover, in all the simulations, the measurements are disturbed by random errors due to instrumental precision. Interruption of signal transmission and abrupt oscillations in the instrument output were also tested. Differently from measurement errors, the lack of signal is easily detected by the control system even without a specific error detection algorithm. Abrupt oscillations are instead quite rare. For these reasons, and for the sake of conciseness, the results of these simulations are not discussed in the following.

Performances of the WSS without application of the validation algorithm

In Figure 5, the performances of the WSS, without the application of the algorithm for fault detection, are shown. In these simulations, one sensor at a time is affected by errors. Three different types of errors are analyzed: (i) drift, (ii) minimum constant value, and (iii) maximum full-scale value. Only the sensors that are essential for the WSS control operations are considered. In Figure 5(a), the *IT* index for the different scenarios is reported. Level and flow rate meters are ranked on the *x* axis according to the *IT* value. For the simulations with $IT = 1$, the sensors are

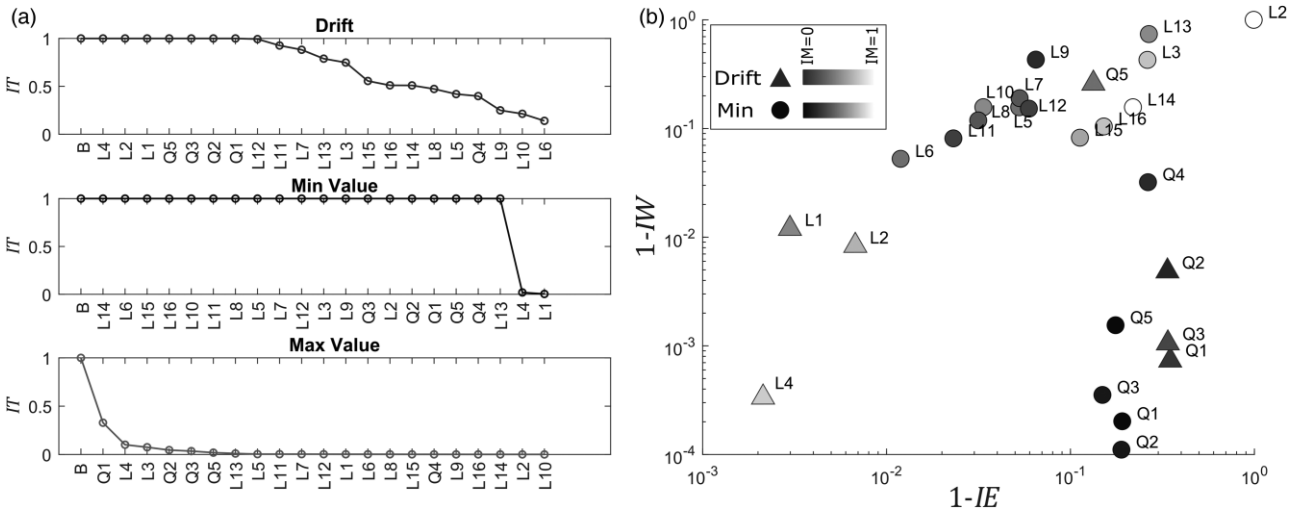

Figure 5 | (a) Normalized time to breakdown (index *IT*) for the three different types of errors. (b) Visualization of the three performance indexes (*IW*, *IE*, and *IM*) for the simulations with $IT = 1$. Circle and triangle markers represent the results for simulations with drift and constant minimum value errors, indexes *IW* and *IE* are reported in the log axes of the chart, while a different shade of the marker fill is assigned according to the mechanical index value (*IM*). Q7

ranked according to the sum of the indexes *IE*, *IW*, and *IM*. In Figure 5(b), the simulations with $IT = 1$ are reported as a function of the three performance indexes *IE*, *IW*, and *IM*. Since the index values are highly concentrated around 1, a better readability is obtained using logarithmic axes of the quantities $1 - IE$ and $1 - IW$, and using a logarithmic scale for the shade of the marker fill that represents the quantity $1 - IM$. In this way, the best scenarios are located near the origin of the axes and present blank markers. The results of the benchmark simulation cannot be visualized on this graph since zero values cannot be represented on a logarithmic scale.

Drift error (first panel in Figure 5(a) and triangle markers in Figure 5(b)) mainly affects level sensors in the municipal tanks. In fact, level sensors L_1 to L_{16} are characterized by $IT < 1$. Based on the drifted level signal, the water level in the tank is overestimated by the SCADA and thus the water flow to the tank from both the water main or the local wells is under-rated and insufficient to match local water consumptions. Drift errors in the level sensors of the four inline tanks (L_1 to L_4) are less critical and jeopardize the system operations only in the long term. In particular, sensors L_1, L_2, and L_4 are rather resilient and their performances are comparable with the benchmark case (see Figure 5(b)). Regarding flow rate sensors, no criticalities are evident except for Q_4, that is, the flow meter involved in the regulation of the T_2 turbine and thus in the regulation of the water level in S_2. This tank is characterized by the smallest volume compared to the other inline tanks, so it is more vulnerable to errors in flow rate measurements. Considering the performances of the WSS under the effect of drifted flow rate measurements to the municipal tanks of the upper valley (Q_1, Q_2, and Q_3), an overestimated flow rate induces a reduction of the flow discharged by the turbines (see Equation (3)), a lower hydroelectric production and thus a decrease of the *IE* index. Moreover, the flow rate balances that govern the opening and closing operations of the turbines are altered and thus a decrease of *IM* index is also observed.

When the faulty sensor settles to the minimum constant value (second panel in Figure 5(a) and circle markers in Figure 5(b)), the WSS operation is generally not compromised. A wrong minimum level in the municipal water tanks (L_5 to L_{16}) entails an excessive water inflow from the local wells and thus a greater energy consumption by the pumping plants and water loss due to water overflowing from the tank. For these reasons, both the *IW* and *IE* indexes greatly decrease (Figure 5(b)). However, critical emptying of the municipal tanks does not occur. On the other hand, inline tanks are more vulnerable to this kind of error since emergency water supply from local wells is not provided. Based on a wrong minimum water level in tanks $S_1(S_2)$, the SCADA system forces a complete closure (see the 'Case study' section) of turbine $T_1(T_2)$ thus impeding the water supply of the downstream tank $S_2(S_3)$. Given its size, tank S_2 is emptied when this error arises in sensor L_1. Similarly, when a minimum level is measured in tank S_4, turbine T_3 is completely opened and the upstream tank S_3 is critically emptied. For these reasons, L_1 and L_4 show the highest vulnerability to this kind of error. A decrease of *IE* and *IM* indexes is observed for errors in the flow rate measurements that disturb the flow rate balances for the regulation of turbine operations (Q_1, Q_2, and Q_3 in Figure 5(b)).

Errors inducing wrong full-scale measurements of level or flow rate in the devices are the most critical for the remote-control system. In municipal tanks, if the level meter indicates that the tank is full, then the tank is not supplied either from the WSS water main or from local sources, and it quickly empties. In inline tanks, based on a wrong maximum level in S_1 and $S_2(S_4)$, the SCADA forces the complete opening(closure) of turbine T_1 and $T_2(T_3)$. Consequently, tanks S_1, S_2, and S_4 are rapidly emptied. When a faulty maximum level is measured in S_3, the water availability in the WSS is overestimated, the municipal tanks are excessively supplied, and thus, the water level in S_3 rapidly decreases. Flow rate sensors are involved in the regulation of the turbine operations and they also exhibit a high vulnerability to this kind of error.

The simulation results shown in Figure 5 evidence the vulnerability of level and flow rate gauges to the most common types of errors. Moreover, the analysis of the performance indexes in Figure 5(b) underlines that even if the system does not reach breakdown, errors still lead to significant worsening in the economic, energy, and mechanical performance of the infrastructure. In particular, it is interesting to observe two main trends in the graph. The simulations related to errors in the level sensors are distributed along the

bisector, indicating a similar deterioration both for the *IW* index and for the *IE* index. The simulations of errors in flow rate sensors, on the other hand, are distributed along a vertical line, indicating that the main consequence is a decrease in energy (and mechanical, if the intensity of the marker fill is observed) performances.

Application of the validation algorithm

After the analysis of the WSS vulnerability to faults in sensors, the above-presented algorithm for real-time fault detection and measurement selection was integrated in the control model of the WSS. First, the available gauges in the different districts of the WSS were checked (hardware redundancy). Second, the balance equations that provide an additional value of the measured physical variables were written (analytical redundancy). Third, for each one of the considered sensors, the algorithm reported in Figure 1 was coded. Finally, different error scenarios were simulated to evaluate the efficiency of the integration in the control model of the error detection algorithm.

To show in detail how the control system operates, Figure 6 reports the results for the assessment of level measurement for the inline tank S_1. Figure 6(a) shows the redundant signals of the tank water level. Figure 6(b) depicts the results of error assessment by the fault detection algorithm.

As introduced in Figure 3(a), two level sensors are installed in each inline tank (MH_1 and MH_2 in Figure 3(a)), providing hardware redundancy. A third value of the tank level is obtained using a mass balance equation of the flow rate into and out of the tank, measured by sensors MQ_{IN} and MQ_{OUT} (Figure 3(a)). The combination of hardware and analytical redundancy guarantees three simultaneous measurements of the same physical variable.

In the exemplifying scenario reported in Figure 6, the level sensor MH_1 (continuous line in Figure 6(a), 6(c), 6(d) and 6(e)) is affected by multiple consecutive errors: (1) drifts, (2) minimum and (3) full-scale constant values, (4) abrupt oscillations, and (5) transmission interruption. The level sensor MH_2 (dotted line in Figure 6(a), 6(c), 6(d) and 6(e)) and the flow rate sensors MQ_{IN} and MQ_{OUT} operate correctly instead, and they are only disturbed by slight random errors due to instrumental precision (Figure 6(e)). Notice that, instrumental errors in the flow rate sensors scarcely affect the precision of the level value (dashed line in Figure 6(e)) obtained from the balance equation.

As shown in Figure 6(a), the level measured by sensor MH_2 is almost equal to the value resulting from the balance equation. On the other hand, the level acquired by MH_1 considerably differs from the previous ones, due to instrumental failures. By means of the residual analysis, the developed algorithm detects with high precision these failures. Figure 6(c) shows in detail the early detection of the drift error. In the first panel, the three curves are very closed one to each other. However, residuals R_1 and R_3, in the second and fourth panels, exceed their respective tolerance thresholds represented by the dashed lines. As a consequence, MH_1 is marked as faulty in the last panel. In Figure 6(b), the outcomes of this error detection procedure are highlighted for all the simulation time. Besides error detection, the algorithm selects in real-time the most reliable measurement (Figure 6(b) and 6(c)) to be used in the WSS control operations. Under ordinary conditions, the algorithm alternatively selects the value measured by one of the two level sensors MH_1 and MH_2. In case of error detection for MH_1, the measurement transmitted by MH_2 is the only one to be selected. As shown in Figure 6(b), the level value obtained from the balance equation is never identified as erroneous because the flow meters involved in the balance operate correctly. Furthermore, the value is never selected by the algorithm as the reference datum for the control operations. In fact, the direct measurements from level sensor MH_1 and MH_2 are always favored to the indirect one. In any case, the level measurement obtained from the balance is fundamental for the operation of the error identification algorithm as it guarantees the triple redundancy on which the algorithm is based.

Performances of the WSS with application of the validation algorithm

The simulations of the response of the system to faulty sensors, discussed above and reported in Figure 5, were performed again. This time, the algorithm for the identification of measurement errors was introduced into the control system. As for the previous analysis, for each one of the considered level and flow rate measurements, three

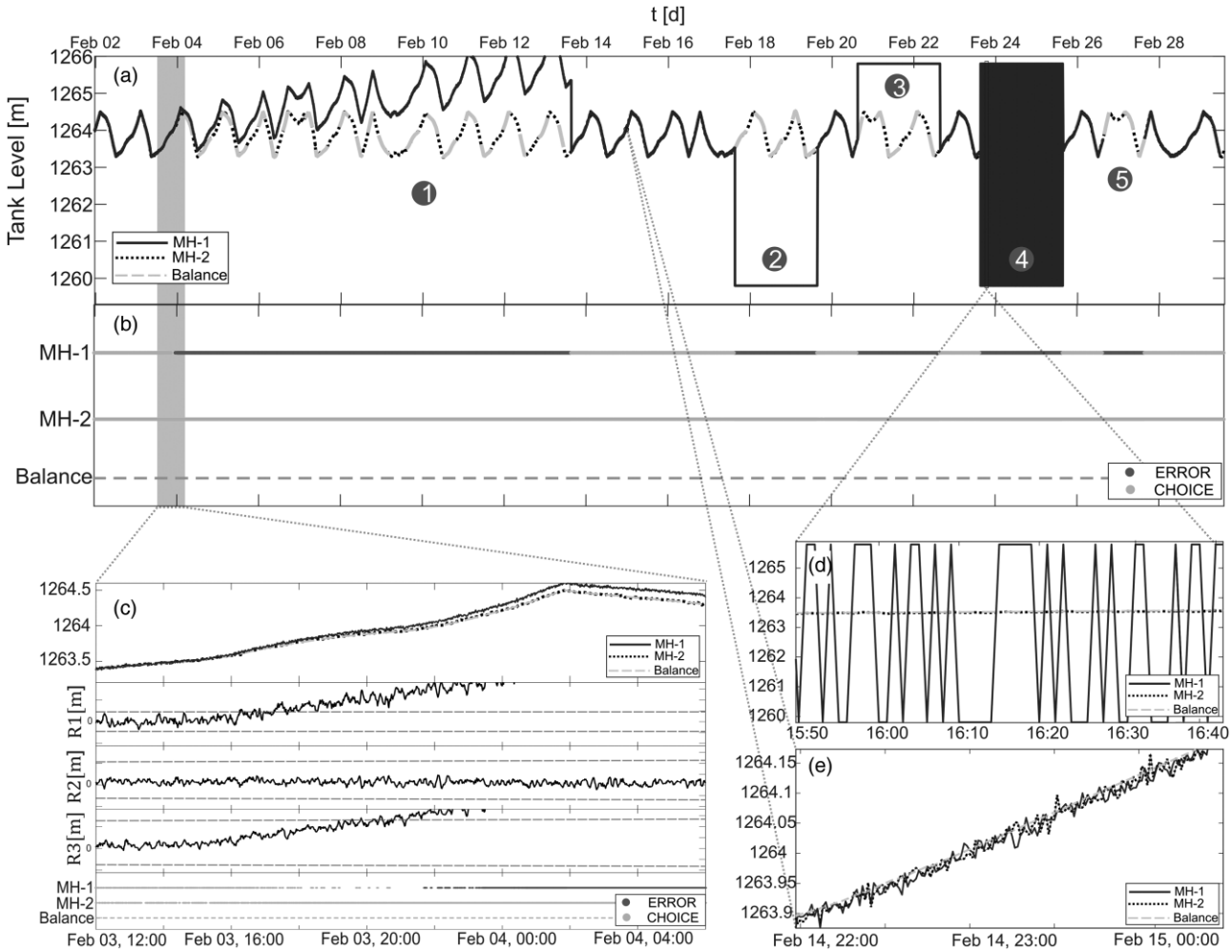

Figure 6 | (a) Level values from level sensors MH_1 (continuous line) and MH_2 (dotted line) and from the balance equation of flow rate into and out of the tank (dashed line). Measurements transmitted by MH_1 experience (1) drifts, (2) minimum and (3) full-scale constant values, (4) abrupt oscillations, and (5) transmission interruptions. (b) Error detection and measurement selection by the fault detection algorithm. (c) Zoom of the early detection of the drift error. As in Figure 4, the three residuals R_1, R_2, and R_3 are reported with the extremes of their tolerance ranges (dashed lines). (d) Zoom of the abrupt oscillations (4). (e) Zoom of the signal showing errors due to instrumental precision.

simulations were conducted. The main sensor was disturbed by (i) drift, and (ii) faulty full-scale and (iii) minimum constant values. Precision errors were simulated for the second redundant sensor and for the sensors involved in the indirect quantification of the third redundant measurement. For each scenario, the WSS dynamics were reproduced for a period of one month.

Results show that in all the simulated scenarios, the algorithm accurately identifies errors in sensors and transmits reliable measurements to the remote-control system. In this way, adjustments of the control devices (turbines and valves) are regularly managed and critical situations that compromise the safety of the aqueduct are prevented. The positive feedback of the system to the introduction of the fault detection algorithm is at first assessed observing that the *IT* index is equal to 1 for all the error scenarios. This indicates that the WSS operates without criticalities for the entire duration of the simulation. However, the *IT* index is not enough to evaluate the improvement of the system performance for the scenarios in which the WSS proved to be resilient even in the absence of the error identification algorithm (i.e., scenarios with $IT = 1$ in Figure 5(a)). For these cases, we calculated the difference between the *IE*, *IW*, and *IM* performance indexes after

and before the introduction of the fault detection procedure (Figure 7).

Results reveal a general increase in the energy index (Δ_{IE}), in particular when errors are detected in the flow rate sensors (Q_1 to Q_5). In fact, the correct regulation of the flow rate through the turbines guarantees the optimization of the hydroelectricity production.

Water saving (Δ_{IW}) is enhanced when the error detection algorithm is applied to level sensors. The water level is the control parameter for the flow rate towards the tanks. When levels are properly measured, the excessive supply of water for the inline and municipal tanks is avoided, thus limiting overflow conditions.

The mechanical index (Δ_{IM}) significantly increases when the signal from the flow rate sensors is verified. As mentioned in Equation (3), these measurements are involved in the balance equations that control the flow rate through the turbines. When the flow rate sensors are faulty, these water balances are only met at the monitoring level but not in the hydraulic system. This results in continuous adjustments of the flow through the turbines. Conversely, when flow rate measurements are assessed, the number of turbine operations is minimized. The implementation of the algorithm induces instead a slight decrease in the mechanical index, when level sensors are stuck on the minimum value (circle markers for level sensors in Figure 7(c)). However, this decrease proves that the WSS is operating properly. In fact, as discussed in the 'Case study' section, when a minimum constant value is erroneously measured in one of the municipal tanks, the control system automatically supplies the tank with an emergency constant flow rate from the water main. Due to this constant flow rate, the natural variation of water supply given by consumptions in the municipalities is reduced, as well as the adjustments of the flow rate through the turbines. When level sensors in the inline tanks are stuck on the minimum constant value, turbines are either completely open or completely closed. Therefore, in these cases, the control operations of the WSS are less dynamic, the number of turbine maneuvers decreases, but also the energy and water saving performances evidently worsen. In fact, a negative Δ_{IM} index is always followed by positive Δ_{IE} and Δ_{IW} indices.

DISCUSSION AND CONCLUSIONS

In this work, an algorithm is proposed for real-time assessment of data measured in the SCADA system of modern and multipurpose WSSs. An automated remote-control system based on reliable flow rate and level measurements is crucial for the safe and optimal operations of these water infrastructures. The developed algorithm compares redundant data provided by both redundant sensors and analytical models. By means of the analysis of residuals, failures and gross errors in sensors are detected. Moreover, the algorithm performs a real-time selection of the most reliable measurements to be used in the control operations.

The effectiveness of the method was assessed through numerical simulations of a coupled hydraulic and control model of an alpine WSS, taken as case study. The considered WSS is currently under construction and thus real datasets from sensors are not available. However, the most common measurement errors have been carefully simulated, based on the technical specifications of the sensors most

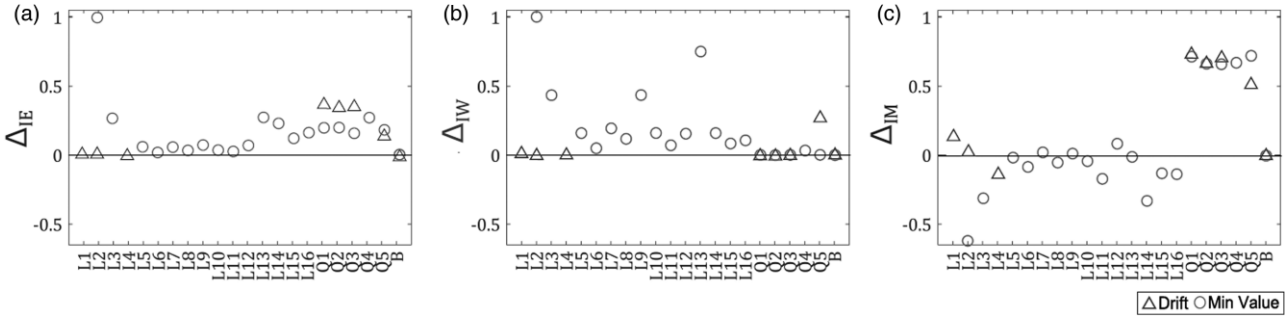

Figure 7 | Increment of the performance indices *IE* (a), *IW* (b), and *IM* (c) after the introduction of the fault detection algorithm in the control system of the WSS. Triangle (circle) markers report the results of simulations with drift (constant minimum value) errors in the sensors.

frequently installed in modern WSSs. By means of these simulations, the system vulnerability to different types of errors in sensors was first analyzed. Four performance indices were defined to assess the achievement of safety, energy, mechanical and water supply targets of the water infrastructure in the different scenarios. Results showed that in most cases, errors in sensors critically undermine the operation of the WSS. Moreover, the most vulnerable sensors were clearly identified. Then, the proposed algorithm was introduced in the control model. The simulations revealed that the algorithm ensures error detection with a high degree of accuracy and guarantees continuity in the system operations. As a result, the performance indices showed a noticeable increase.

The developed algorithm is robust and easy to implement. Moreover, the proposed tools for modeling the hydraulic behavior of the WSS, its control system, and sensor errors are useful to carry out preliminary studies on the performance and safety of a WSS in the design phase. Within this approach, hardware redundancy can be optimized.

The algorithm can verify the reliability of a control variable only in the case of a single faulty sensor among those involved in the estimation of the three redundant estimates of the variable. In the event of multiple, simultaneous errors the algorithm is not effective. Also, water leaks can disturb the hydraulic balances involved in the analytically redundant measurements. In this case, if the corresponding sensors (hardware redundancy) are not faulty, the algorithm identifies the presence of an error in the hydraulic balance and can thus help in localizing water leaks. Once detected, water leaks must be fixed, or the balance equation implemented in the algorithm must be modified to take these outflows into account. If one of the two redundant sensors is out of order, the unexpected occurrence of water leaks precludes the correct functioning of the algorithm. At the state-of-the-art, the method therefore requires that in the event of a sensor malfunction, a maintenance intervention on site is arranged in a short time so as to prevent a second failure being added to the first one. Another aspect to be considered for the application of the proposed FDI in real WSSs is the frequency for sensor data validation. The fault detection algorithm should assess data with a frequency that is in line with the measurement frequency of the sensors, and with the speed of the WSS dynamics. All these aspects, i.e., the frequency of sensor maintenance, in-site human intervention, and data validation, are case-dependent and should be examined during the design of the control and fault detection system.

ACKNOWLEDGMENTS

We gratefully acknowledge SMAT Group for the financial support to this research and for providing valuable information.

REFERENCES

Anghileri, D., Castelletti, A., Pianosi, F., Soncini-Sessa, R. & Weber, E. 2012 Optimizing watershed management by coordinated operation of storing facilities. *Journal of Water Resources Planning and Management* **139** (5), 492–500.

Balaban, E., Saxena, A., Bansal, P., Goebel, K. F. & Curran, S. 2009 Modeling, detection, and disambiguation of sensor faults for aerospace applications. *IEEE Sensors Journal* **9** (12), 1907–1917.

Bel, G. & Warner, M. E. 2015 Inter-municipal cooperation and costs: Expectations and evidence. *Public Administration* **93** (1), 52–67.

Boukhris, A., Giuliani, S. & Mourot, G. 2001 Rainfall–runoff multi-modelling for sensor fault diagnosis. *Control Engineering Practice* **9** (6), 659–671.

Burnell, D. 2003 Auto-validation of district meter data. In: *Proceedings of the CCWI'03 Conference In Advances in Water Supply Management*, 15–17 September, London, UK, pp. 13–22.

Carrera, L., Mysiak, J. & Crimi, J. 2013 Droughts in Northern Italy: Taken by Surprise, Again. *Review of Environment, Energy and Economics (Re3)*.

Casillas, M., Puig, V., Garza-Castañón, L. & Rosich, A. 2013 Optimal sensor placement for leak location in water distribution networks using genetic algorithms. *Sensors* **13** (11), 14984–15005.

Chen, J. & Patton, R. J. 2012 *Robust Model-based Fault Diagnosis for Dynamic Systems*. Springer Science & Business Media 3.

Ciavatta, S., Pastres, R., Lin, Z., Beck, M. B., Badetti, C. & Ferrari, G. 2004 Fault detection in a real time monitoring network for water quality in the lagoon of Venice (Italy). *Water Science and Technology* **50** (11), 51–58.

Coelho, B. & Andrade-Campos, A. 2014 Efficiency achievement in water supply systems-A review. *Renewable and Sustainable Energy Reviews* **30**, 59–84.

Cugueró-Escofet, MÀ, Quevedo, J., Alippi, C., Roveri, M., Puig, V., García, D. & Trovò, F. 2016 Model-vs. data-based approaches

applied to fault diagnosis in potable water supply networks. *Journal of Hydroinformatics* **18** (5), 831–850.

EC (European Communities) 2000 *Directive 2000/60/EC of the European Parliament and of the Council Establishing a Framework for Community Action in the Field of Water Policy*. OJ L327, 22.12.2000.

Eliades, D. & Polycarpou, M. 2010 A fault diagnosis and security framework for water systems. *IEEE Transactions on Control Systems Technology* **18** (6), 1254–1265.

Fellini, S., Vesipa, R., Boano, F. & Ridolfi, L. 2017 Multipurpose design of the flow-control system of a steep water main. *Journal of Water Resources Planning and Management* **144** (2), 05017018.

Fellini, S., Vesipa, R., Boano, F. & Ridolfi, L. 2018 Real-time measurement fault detection and remote-control in a mountain water supply system. In: *HIC 2018. 13th International Conference on Hydroinformatics*, Vol. 3 (G. La Loggia, G. Freni, V. Puleo & M. De Marchis eds), pp. 698–705.

Frank, P. M. 1996 Analytical and qualitative model-based fault diagnosis – a survey and some new results. *European Journal of Control* **2** (1), 6–28.

Frank, P. M. & Ding, X. 1997 Survey of robust residual generation and evaluation methods in observer-based fault detection systems. *Journal of Process Control* **7** (6), 403–424.

Frank, P. M. & Köppen-Seliger, B. 1997 Fuzzy logic and neural network applications to fault diagnosis. *International Journal of Approximate Reasoning* **16** (1), 67–88.

Fuller, W. A. 2009 *Measurement Error Models*. John Wiley & Sons, New York, USA.

Gabrys, B. & Bargiela, A. 1996 Integrated neural based system for state estimation and confidence limit analysis in water networks. In: *Proceedings of European Simulation Symposium ESS'96*, Genoa, pp. 398–402.

Gao, Z., Cecati, C. & Ding, S. X. 2015 A survey of fault diagnosis and fault-tolerant techniques-Part I: Fault diagnosis with model-based and signal-based approaches. *IEEE Transactions on Industrial Electronics* **62** (6), 3757–3767.

Gertler, J. 1988 Survey of model-based failure detection and isolation in complex plants. *IEEE Control Systems Magazine* **8** (6), 3–11.

Gertler, J. 2015 *Fault Detection and Diagnosis*. Springer, London, UK.

Goupil, P. 2011 AIRBUS state of the art and practices on FDI and FTC in flight control system. *Control Engineering Practice* **19** (6), 524–539.

Hwang, I., Kim, S., Kim, Y. & Seah, C. 2010 A survey of fault detection, isolation, and reconfiguration methods. *IEEE Transactions on Control Systems Technology* **18** (3), 636–653.

Isermann, R. 2005 Model-based fault-detection and diagnosis–status and applications. *Annual Reviews in Control* **29** (1), 71–85.

Izquierdo, J., López, P. A., Martínez, F. J. & Pérez, R. 2007 Fault detection in water supply systems using hybrid (theory and data-driven) modelling. *Mathematical and Computer Modelling* **46** (3–4), 341–350.

JCGM J 2008 Evaluation of Measurement Data–Guide to the Expression of Uncertainty in Measurements. *Joint Committee for Guides in Metrology*.

Krause, A., Leskovec, J., Guestrin, C., Van Briesen, J. & Faloutsos, C. 2008 Efficient sensor placement optimization for securing large water distribution networks. *Journal of Water Resources Planning and Management* **134** (6), 516–526.

Maki, Y. & Loparo, K. A. 1997 A neural-network approach to fault detection and diagnosis in industrial processes. *IEEE Transactions on Control Systems Technology* **5** (6), 529–541.

Massarutto, A. 2000 *Agriculture, water resources and water policies in Italy*. Fondazione Eni Enrico Mattei, Milano, Italy.

Meseguer, J. & Quevedo, J. 2017 Real-time monitoring and control in water systems. In: *Real-time Monitoring and Operational Control of Drinking-Water Systems*. Springer, Cham, Switzerland, pp. 1–19.

Meseguer, J., Puig, V. & Escobet, T. 2010 Fault diagnosis using a timed discrete-event approach based on interval observers: Application to sewer networks. *IEEE Transactions on Systems, Man and Cybernetics: Part A* **40** (5), 900–916.

Mourad, M. & Bertrand-Krajewski, J. L. 2002 A method for automatic validation of long time series of data in urban hydrology. *Water Science and Technology* **45** (4–5), 263–270.

Özyurt, D. B. & Pike, R. W. 2004 Theory and practice of simultaneous data reconciliation and gross error detection for chemical processes. *Computers & Chemical Engineering* **28** (3), 381–402.

Piatyszek, E., Voignier, P. & Graillot, D. 2000 Fault detection on a sewer network by a combination of a Kalman filter and a binary sequential probability ratio test. *Journal of Hydrology* **230** (3–4), 258–268.

Pukelsheim, F. 1994 The three sigma rule. *The American Statistician* **48** (2), 88–91.

Quevedo, J., Puig, V., Cembrano, G., Blanch, J., Aguilar, J., Saporta, D., Benito, G., Hedo, M. & Molina, A. 2010 Validation and reconstruction of flow meter data in the Barcelona water distribution network. *Control Engineering Practice* **18** (6), 640–651.

Ragot, J. & Maquin, D. 2006 Fault measurement detection in an urban water supply network. *Journal of Process Control* **16** (9), 887–902.

Sharma, A. B., Golubchik, L. & Govindan, R. 2010 Sensor faults: Detection methods and prevalence in real-world datasets. *ACM Transactions on Sensor Networks (TOSN)* **6** (3), 23.

Vesipa, R. & Fellini, S. 2019 Instability of the tank-level control system of water mains in mountainous environments. *Journal of Hydraulic Engineering* **145** (7).

Webster, J. G. 1998 *The Measurement, Instrumentation and Sensors Handbook*. CRC Press, Boca Raton, FL, USA.